nature cell biology

p53 mRNA controls p53 activity by managing Mdm2 functions

Marco M. Candeias[1], Laurence Malbert-Colas[1], Darren J. Powell[1], Chrysoula Daskalogianni[1], Magda M. Maslon[1], Nadia Naski[1], Karima Bourougaa[1], Fabien Calvo[1] and Robin Fåhraeus[1,2]

The E3 ubiquitin ligase Mdm2 is a focal regulator of p53 tumour suppressor activity. It binds p53, promoting its polyubiquitination and degradation, and also controls p53 synthesis. However, it is not known how this dual function of Mdm2 on p53 synthesis and degradation is achieved. Here we show that the *p53* mRNA region encoding the Mdm2-binding site interacts directly with the RING domain of Mdm2. This impairs the E3 ligase activity of Mdm2 and promotes *p53* mRNA translation. We also show that introduction of cancer-derived single silent point-mutations in the *p53* mRNA weakens its binding to Mdm2 and results in reduced p53 activity. These data are consistent with a mechanism by which changes in silent nucleotides can affect the function of the encoded protein, and indicate that Mdm2-mediated control of p53 synthesis and degradation has evolved in the *p53* mRNA sequence and its encoded amino acids.

Binding of Mdm2 to the transcriptional transactivation domain 1 (TD1; ref. 1) in the amino terminus of p53 inhibits the activity of p53 and targets it for proteasomal degradation[2,3]. Mdm2 promotes translation of the full-length p53 ($p53^{FL}$) and the alternative translation product p53/47, which is initiated 40 codons downstream[4] and lacks the Mdm2-binding domain (MBD, residues 15–26; ref. 5).

Recently, it was shown that the MBD-encoding sequence (MBD-ES) of *p53* mRNA can mediate control of *p53* mRNA translation[6,7]. To investigate whether this region is involved in Mdm2-mediated regulation of *p53* translation, we introduced silent mutations in the third positions of codons 17, 18 and 19 of *p53* ($p53^{TriM}$, Supplementary Information, Fig. S1). Expression of the *TriM* message in p53-negative H1299 cells result in lower wild-type p53 protein levels (Fig. 1a). However, in the presence of Mdm2, wild-type p53 expressed from the *TriM* message increased, whereas mRNA levels remained unchanged (Fig. 1a and data not shown). When studied separately, the rates of protein synthesis and degradation were both found to be enhanced in the *TriM* construct in the presence of Mdm2 (Fig. 1a; Supplementary Information, Fig. S2a). The capacity of $p53^{TriM}$ mRNA to enhance Mdm2-dependent p53 synthesis was also observed using an Mdm2 protein that carries a point mutation (C464A), which causes abrogation of its E3 ubiquitin ligase activity[2,8]. This shows that the capacity of Mdm2 to regulate *p53* mRNA translation is not dependent on its E3 ubiquitin ligase capacity (Fig. 1b).

We next looked in data banks for naturally occurring silent mutations in the MBD-ES region of the *p53* gene. The L22L (CTA>CTG) single silent mutation was identified in a human tumour[9] and generates *p53* mRNA that translates p53 at a constant rate in the presence or absence of Mdm2 (Fig. 1c).

These results highlight the importance of *p53* mRNA in Mdm2-mediated control of p53 synthesis and degradation, and we wanted to determine whether the Mdm2–p53 protein interaction is also involved in Mdm2-dependent control of p53 synthesis. To address this question we mutated the first initiation codon in the *TriM* message (M1A). This construct only expresses the p53/47 protein, which lacks the MBD and thus does not interact with Mdm2. However, this mRNA retains the MBD-ES and its susceptibility to Mdm2-dependent induction of mRNA translation (Fig. 1d). In contrast, Mdm2 did not induce translation of *p53* mRNA in which the first 120 encoding nucleotides had been deleted (Δ120; Fig. 1d). However, Mdm2 induced translation of a construct where the first 120 coding nucleotides of p53 had been fused in front of GFP, giving rise to the 120–GFP fusion product, as well as GFP itself (Fig. 1d). We also examined the effects of replacing the first 120 encoding nucleotides in the *p53* mRNA with the 36 nucleotides that encode the core sequence of the MBD (amino acids 15–26, construct MBDp47). As shown by pulse label experiments (Fig. 1e), *MBDp47* mRNA translation could be induced by Mdm2 and the encoded protein was capable of binding Mdm2.

The Mdm2 isoform $p76^{Mdm2}$ lacks the p53 binding domain and cannot target p53 for degradation. $p76^{Mdm2}$ can be generated either through alternative translation initiation or splicing of *Mdm2* RNA, and has been shown to have a positive effect on p53 activity[10,11]. To test whether $p76^{Mdm2}$ promotes p53 synthesis, we expressed $p76^{Mdm2}$ either from an N-terminal deletion construct (Δ1–61, ΔNMdm2) or by substituting the first two AUG codons in the *Mdm2* message with alanine (AA/MMdm2). Both constructs express $p76^{Mdm2}$ (data not shown) and induce a similar 3-fold

[1]Inserm U716, Pharmacologie Expérimentale, Institut Génétique Moléculaire, Hôpital St Louis and Université Paris 7, 27 rue Juliette Dodu, 75010 Paris, France.
[2]Correspondence should be addressed to R.F. (e-mail: robinfahraeus@yahoo.co.uk)

Received 7 March 2008; accepted 4 July 2008; published online 10 August 2008; DOI: 10.1038/ncb1770

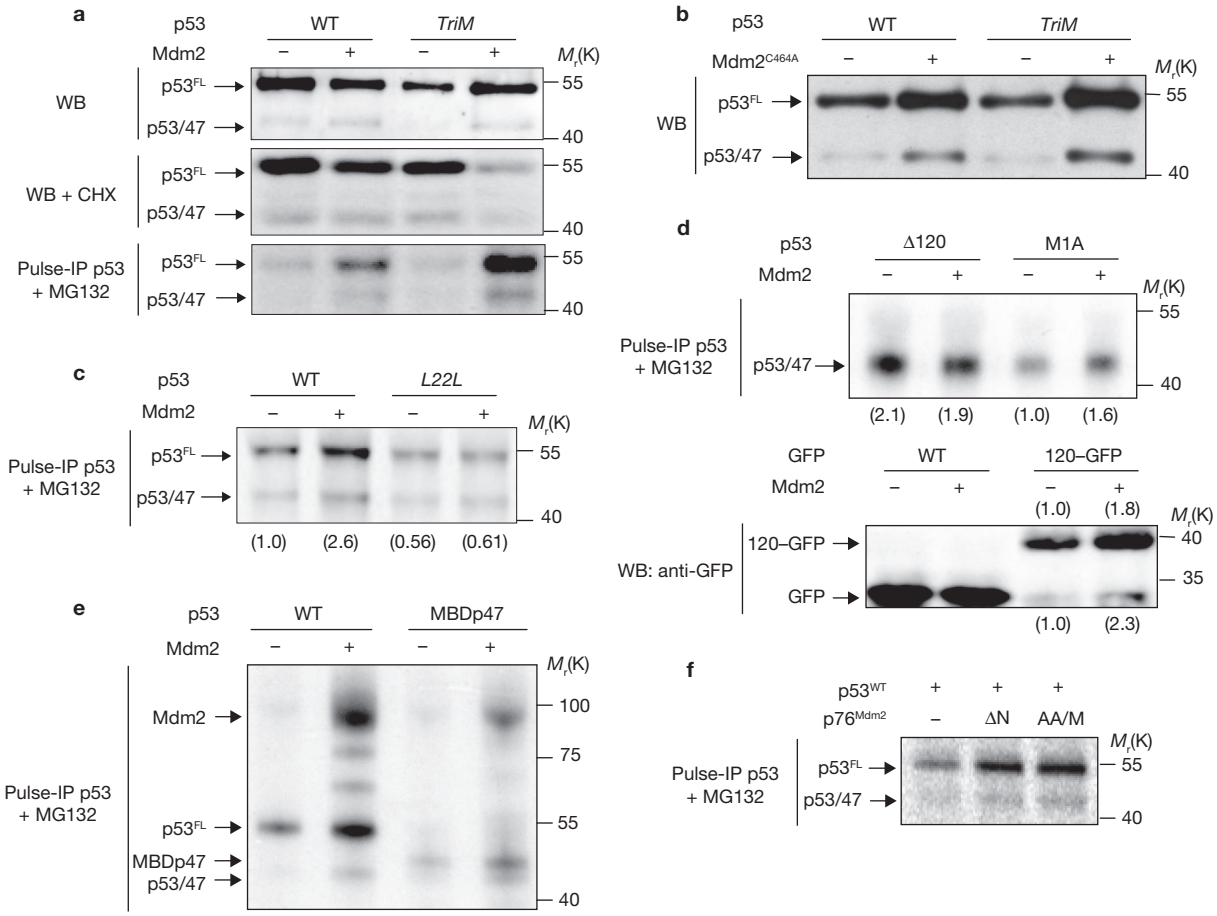

Figure 1 Mdm2-dependent control of *p53* mRNA translation is mediated by the *p53* mRNA sequence (MBD-ES) that encodes the Mdm2-binding domain (MBD). (**a**) Western blot (WB) of wild-type p53 (WT) proteins expressed from different mRNAs in *p53*-null H1299 cells untreated or treated with the protein synthesis inhibitor cycloheximide (CHX). The $p53^{TriM}$ mRNA carries silent mutations in the third positions of codons 17, 18 and 19. A 20 min ^{35}S-methionine metabolic pulse-labelling (Pulse) was performed in the presence of the proteosome inhibitor MG132 (autoradiograph, bottom panel). (**b**) An Mdm2 protein carrying a point mutation ($Mdm2^{C464A}$) that inactivates its E3 ligase activity still induces p53 synthesis. (**c**) Pulse-labelling of p53 from an mRNA carrying a silent mutation found in a human cancer (L22L, CTA>CTG; Supplementary Information, Fig. S1). (**d**) p53/47 is initiated 40 codons downstream of $p53^{FL}$. The $p53^{M1A}$ mRNA carries a mutation in the first AUG codon and $p53^{\Delta 120}$ lacks the first 120 encoding nucleotides (autoradiograph, top). 120–GFP has the first 120-nucleotide sequence encoding the N terminus of p53 fused to GFP (WB, bottom). (**e**) The *p53* mRNA sequence encoding MBD (amino acids 15–26; see Supplementary Information, Fig. S1) of p53 fused directly to Δ120 ($p47^{MBD}$) is sufficient to mediate Mdm2-dependent induction of p53 synthesis. (**f**) The $p76^{Mdm2}$ is derived either from alternative translation initiation sites or splicing of the *mdm2* RNA and lacks the N-terminal p53-binding domain. Expression of $p76^{Mdm2}$ after removing the first 61 codons (ΔN) or mutating the first two AUG codons of *mdm2* mRNA (AA/M) results in the induction of *p53* mRNA translation. The data represent one of four independent experiments. Transfection efficiencies and mRNA expression levels were tested using qRT–PCR. The numbers in parenthesis indicate the relative amounts of each band according to WB quantifications or phosphoimager analysis. CHX treatment was for 1 h.

increase in wild-type *p53* mRNA translation (Fig. 1f). This indicates that the p53–Mdm2 protein–protein interaction is not required for Mdm2-induced *p53* mRNA translation, and also offers an explanation for the positive role of $p76^{Mdm2}$ on p53 activity. These results indicate that the MBD-ES region in *p53* mRNA, but not the Mdm2–p53 protein interaction, is sufficient and necessary to sustain Mdm2-dependent induction of *p53* mRNA translation, and that the capacity of Mdm2 to control the rate of p53 synthesis and degradation have developed on the same *p53* genomic sequence.

As Mdm2 has previously been shown to be in complexes with ribosomal RNA[12], and to have RNA-binding capacity *in vitro*[13], we next tested whether Mdm2 interacts directly and specifically with *p53* mRNA. The amount of wild-type, $p53^{L22L}$ or $p53^{TriM}$ mRNAs that immunoprecipitated with Mdm2 was determined using quantitative real-time RT–PCR (qRT–PCR) in H1299 cells. After normalization to Mdm2 protein and total RNA levels, the amount of *TriM* mRNA that co-immunoprecipitated with Mdm2 was found to be 2.5-fold higher than with wild-type mRNA. On the other hand, the quantity of $p53^{L22L}$ mRNA that associated with Mdm2 was only slightly higher than that of the TATA-binding protein (TBP) control mRNA, and similar to transfected *p21* mRNA (Fig. 2a).

To determine which part of Mdm2 mediates the interaction with *p53* mRNA, we analysed the capacity of a series of truncated and mutated Mdm2 proteins to interact with *p53* mRNA. For this purpose we used a non-encoding $p53^{TriM}$ in which all three translation initiation sites[4] have been mutated (silent TriM or $p53^{STriM}$) (Fig. 2b; Supplementary Information, Fig. S1b). Deletion of the RING domain of Mdm2 (Δ410–489, ΔC), including the E3 ubiquitin ligase catalytic site of

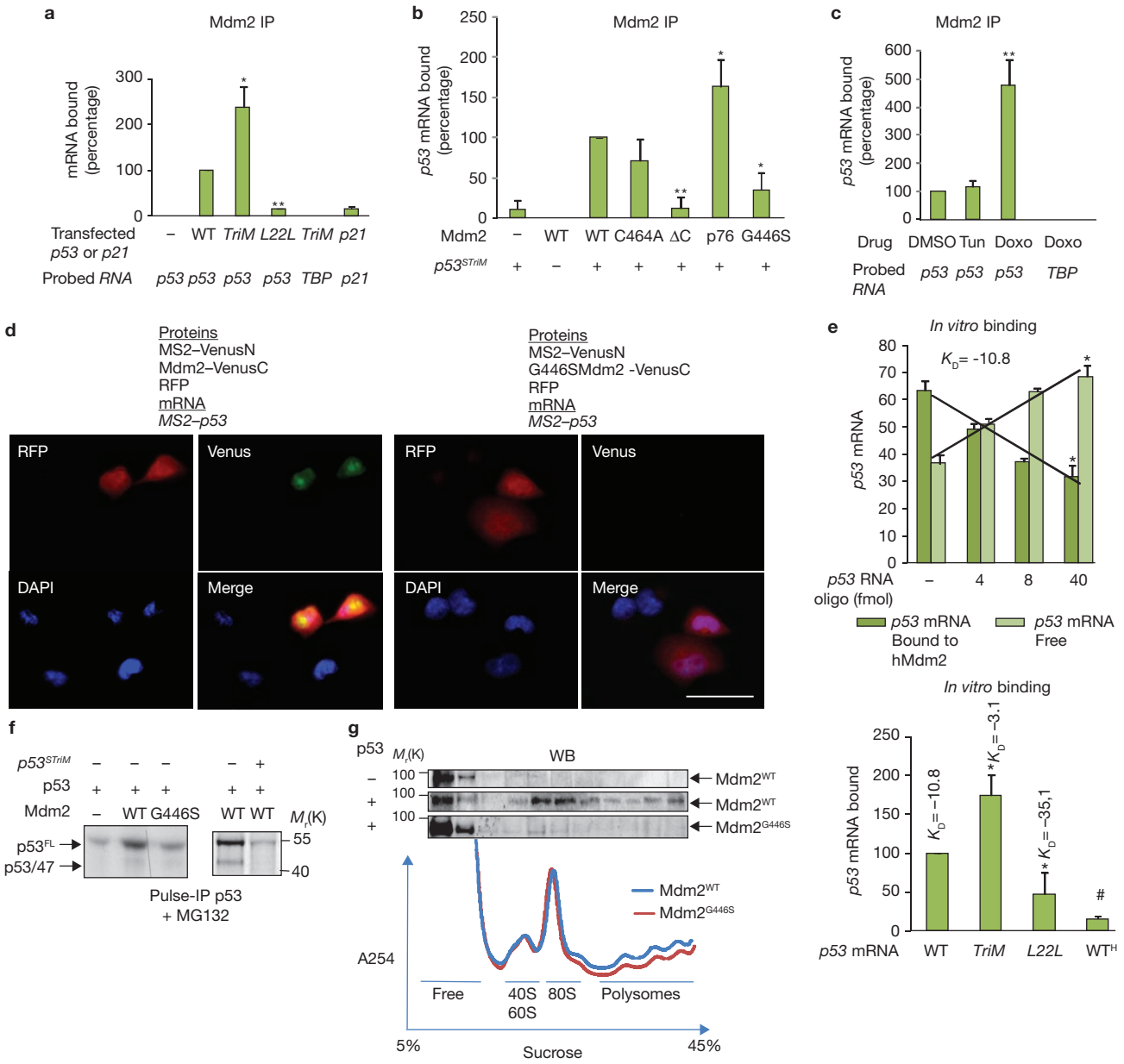

Figure 2 Mdm2 interacts directly and specifically with the MBD-ES of *p53* mRNA to induce *p53* translation. H1299 cells were transfected with the indicated constructs. (**a**) The relative amounts of *p53*, TATA-binding protein (TBP) and overexpressed *p21* mRNAs co-immunoprecipitating with Mdm2 are shown. (**b**) The *STriM* mRNA carries mutations in all initiation codons and does not express p53 protein (Supplementary Information, Fig. S1). The $Mdm2^{G446S}$ does not bind RNA[12]. (**c**) Binding of Mdm2 to *p53* or *TBP* mRNAs after treatment with doxorubicin (0.1 μM) or tunicamycin (1.2 μM). (**d**) The N-terminal half of Venus fluorescent protein was fused to the MS2 peptide (MS2–VenusN) and the C-terminal half to the C-terminus of Mdm2 (Mdm2–VenusC). The MS2 peptide-binding RNA sequence is introduced to the 5′-untranslated region (5′-UTR) of *p53* mRNA (MS2–p53). The binding of Mdm2 and MS2 peptide to *p53* mRNA brings the two halves of Venus close to each other, generating a fluorescent product (left). DAPI marks cell nuclei (blue) and red fluorescent protein (RFP) marks transfected cells (red) (see also Supplementary Information, Fig. S4a). Scale bar, 40 μm. (**e**) *In vitro*-transcribed *p53* mRNA (8 fmol) was incubated with recombinant purified hMdm2 (120 ng) and tRNA (5 μg), and increasing amounts (0–40 fmol) of the MBD-ES RNA oligonucleotide were added. The quantity of free and Mdm2-bound *p53* mRNA was estimated using qRT–PCR and the dissociation constants calculated (K_D). WT^H is pre-heated wild-type *p53* mRNA. (**f**) Pulse-labelling shows the effect of wild-type Mdm2 and $Mdm2^{G446S}$ proteins, and $p53^{STriM}$ mRNA on p53 synthesis. (**g**) WB shows the association of Mdm2 with polysomal fractions. The localization of mRNPs, monosomes and polysomes are indicated (bottom). For panels **d**, **f** and **g**, one representative experiment of four independent experiments is shown. For panels **a**–**c** and **e**, data are means ± s.d. of three independent experiments (*$P < 0.05$, **$P < 0.01$, #$P < 0.005$, ##$P < 0.001$). *P* values are compared with wild-type p53 (**a**), wild-type Mdm2 (**b**), DMSO-treated (**c**), no oligonucleotide (**e**, top) and wild-type *p53* mRNA (**e**, bottom).

Mdm2, abolished the capacity of Mdm2 to interact with *p53* mRNA. In contrast, deletion of the Mdm2 N terminus ($p76^{Mdm2}$) resulted in an increase in the amount of mRNA that co-immunoprecipitated with Mdm2. Introduction of a point mutation in codon 446 (G446S; in the Mdm2 RING domain), previously shown to prevent Mdm2 from binding non-specific RNA oligonucleotides[13], also reduced the specific *p53* mRNA-binding capacity of Mdm2 without altering its p53 protein-binding ability (Fig. 2b; Supplementary Information, Fig. S3a). The

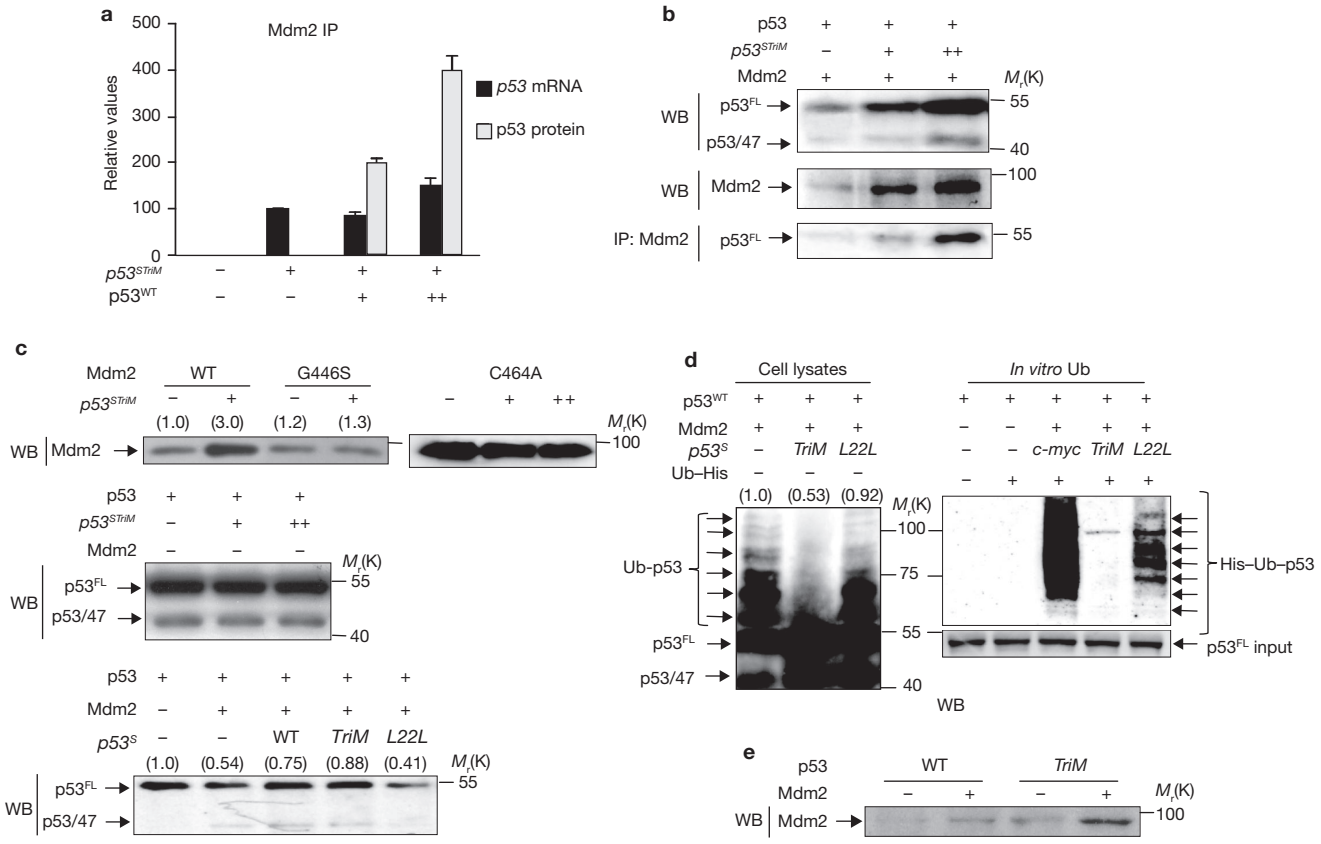

Figure 3 *p53* mRNA controls Mdm2 E3 ubiquitin ligase activity. (**a**) H1299 cells were transfected with Mdm2 and the indicated p53 constructs. The amount of $p53^{STriM}$ mRNA that co-immunoprecipitated with Mdm2 was assessed using qRT–PCR after normalization to total RNA and Mdm2 levels (black bars). The grey bars represent total p53 protein levels as determined by WB. Increasing amounts of p53 protein did not prevent Mdm2 from co-immunoprecipitating with *p53* mRNA. (**b**) Increasing amounts of $p53^{STriM}$ mRNA caused an increase in p53 and Mdm2 expression levels (top and middle panels) but did not affect the capacity of Mdm2 to co-immunoprecipitate with p53 protein (bottom panel). (**c**) $p53^{STriM}$ mRNA increased the levels of wild-type Mdm2 but had no effect on the expression levels of the non-RNA binding $Mdm2^{G446S}$ (top left panel) or on the levels of the E3 ligase inactive $Mdm2^{C464A}$ (top right) or p53 levels (middle panel). The silent wild-type and $p53^{STriM}$, but not the $p53^{SL22L}$ mRNAs, stabilize p53 in the presence of Mdm2 (bottom panel). (**d**) Expression of *STriM*, but not *SL22L*, mRNAs prevents p53 polyubiquitination in H1299 cells (left panel). Blockade of hMdm2-dependent ubiquitination of p53 *in vitro* by *in vitro*-transcribed *STriM* mRNA was more effective than that caused by *SL22L* mRNA or the control *c-myc* mRNA (right panel; see also Supplementary Information, Fig. S5). The amount of *in vitro* His-ubiquitinated p53 products is shown by WB using anti-His monoclonal antibodies (**e**) WB shows that the levels of Mdm2 increase in the presence of $p53^{TriM}$ mRNA. For panels **b**–**e**, one representative experiment of four independent experiments is shown. For panel **a**, data are means ± s.d. of three independent experiments. Transfection efficiencies and mRNA expression levels were tested using qRT–PCR. The numbers in parenthesis indicate the relative amounts of each band (except for polyubiquitination data, where each number indicates the relative amounts of all the polyubiquitinated p53 bands together) according to WB quantifications or phosphoimager analysis.

C464A E3-ligase-impaired Mdm2 retained approximately 70% of the binding capacity of wild-type Mdm2.

When we treated cells expressing *Mdm2* and $p53^{STriM}$ mRNA with doxorubicin, a chemical inducer of DNA damage and a well known activator of the p53 pathway, we observed an increase of about 5-fold in the association between *p53* mRNA and Mdm2 (Fig. 2c). In contrast, tunicamycin treatment, which induces the unfolding stress response, had little effect. Hence, the Mdm2–*p53* mRNA interaction is subject to cellular control by DNA damage response pathways.

To visualize a direct interaction between the *p53* mRNA and Mdm2 in cells, we used trimolecular fluorescence complementation (TriFC)[14]. We inserted a known RNA sequence (MS2 site) in the 5′-UTR of the *p53* message. This sequence binds the bacteriophage MS2 coat peptide, which had been cloned to the N-terminal half of a Venus fluorescent protein[15] (MS2–VenusN). The complementary part of Venus was fused in the C-terminal end of Mdm2 (Mdm2–VenusC). Binding of Mdm2–VenusC and MS2–VenusN to *p53* mRNA brought the two Venus regions together and revealed a fluorescent product. Introduction of the G446S mutation in Mdm2–VenusC or the L22L mutation in the *p53* mRNA prevented the formation of the trimolecular complex (Fig. 2d; Supplementary Information, Fig. S4a).

We also observed a direct Mdm2–*p53* mRNA interaction *in vitro* by performing binding assays in which we used increasing amounts of a biotinylated RNA oligonucleotide corresponding to the MBD-ES, to compete with different *in vitro* transcribed *p53* mRNAs for binding to purified recombinant human Mdm2 (hMdm2; Fig. 2e). In addition, we performed gel retardation assays in which we used *p53* mRNA instead as a competitor for the biot-RNAoligo–hMdm2 interaction (Supplementary Information, Fig. S4b). These different assays showed that $p53^{\Delta 120}$ and $p53^{L22L}$ mRNAs have only a weak affinity for Mdm2 and that $p53^{TriM}$ mRNA has a stronger affinity for Mdm2, compared with wild-type mRNA. Heat-treated wild-type *p53* mRNA did not bind

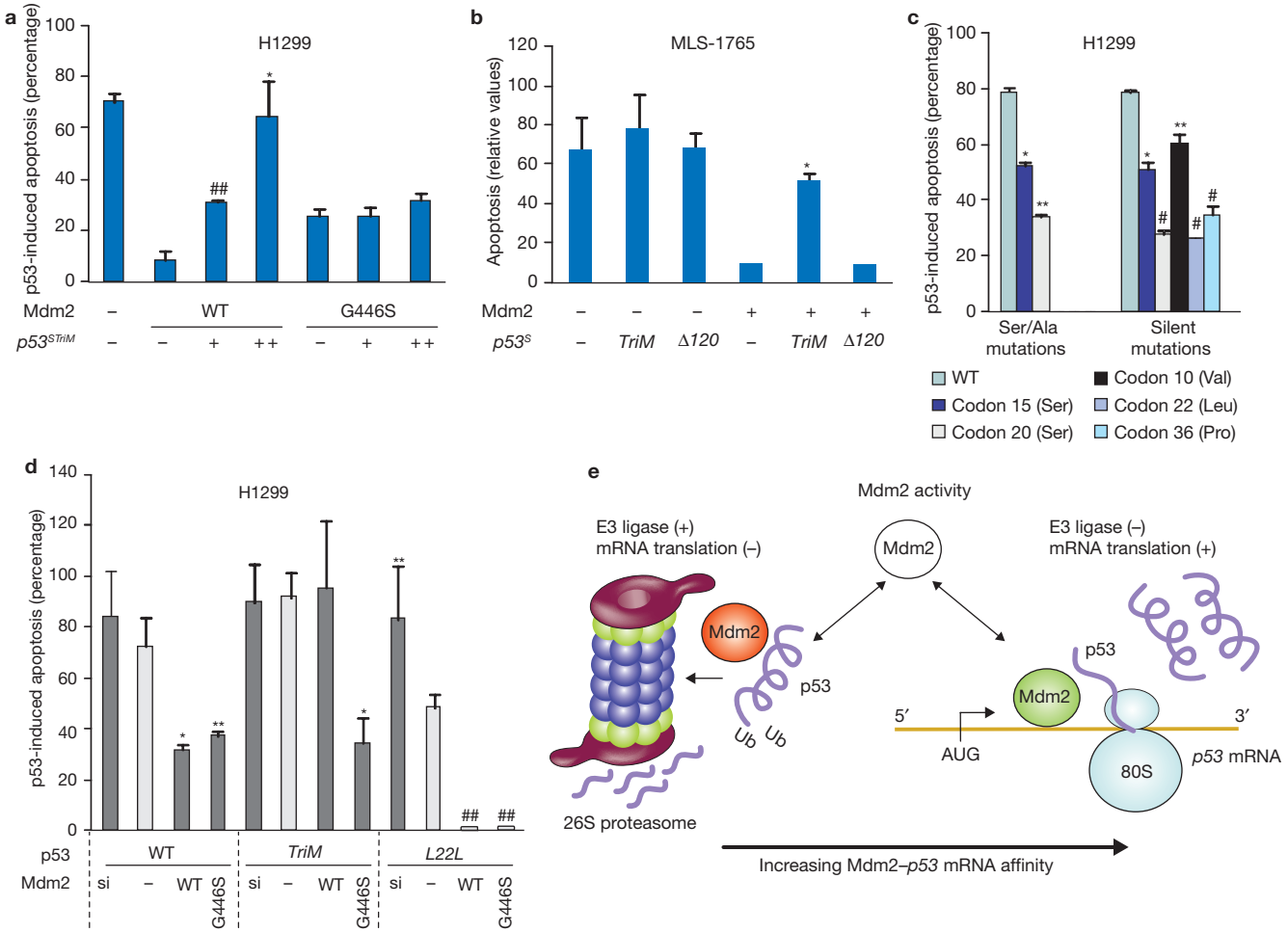

Figure 4 The Mdm2–*p53* mRNA interaction controls p53 activity. (**a**) The graph shows p53-induced apoptosis in H1299 cells expressing wild-type p53 and the indicated constructs. $p53^{STriM}$ mRNA did not affect the capacity of the non-RNA binding $Mdm2^{G446S}$ mutant to suppress p53-induced apoptosis. (**b**) MLS-1765 cells express endogenous wild-type p53. $p53^{STriM}$ mRNA, but not $p53^{S\Delta120}$ mRNA, prevented Mdm2-dependent reduction in apoptosis. The data are normalized to the level of apoptosis in Mdm2-transfected cells (10%). (**c**) The role of *p53* mRNA, compared with the encoded peptide, on p53 activity was tested. The S15S and S20S silent mutants mimic the changes in the MBD-ES structures induced by the mutations S15A and S20A, respectively (see Supplementary Information, Fig. S1a), and have the same effect on p53-dependent apoptosis. Three single silent cancer-derived mutations (V10V, L22L and P36P) were tested. These mRNAs have lower affinity for Mdm2 and express lower levels of wild-type p53 protein (Supplementary Information, Fig. S5). (**d**) *p53* mRNA-mediated control of p53-induced apoptosis. siRNA (si) and overexpression (wild-type or $Mdm2^{G446S}$) were used to minimize or increase Mdm2 levels (see Supplementary Information, Fig. S3b). The affinity of *p53* mRNA for Mdm2 directs Mdm2 control of p53-induced apoptosis. Expression of the non-RNA binding $Mdm2^{G446S}$ prevented p53 activity from all mRNAs. (**e**) A model illustrating how the binding of Mdm2 to *p53* mRNA can switch Mdm2 function towards p53. Binding of *p53* mRNA to Mdm2 induces p53 synthesis and prevents Mdm2 E3 ubiquitin ligase activity (right). Low mRNA-Mdm2 affinity, as observed with the cancer-derived mutants, results in Mdm2 becoming a more effective repressor of p53 activity (left). For panels **a**–**d**, data are means ± s.d. of three independent experiments ($*P < 0.05$, $**P < 0.01$, $\#P < 0.005$, $\#\#P < 0.001$). *P* values are compared with wild-type Mdm2 plus no $p53^{STriM}$ (**a**, **b**), wild-type p53 (**c**) and the different endogenous Mdm2 conditions (**d**, light bars). The flow cytometry data using H1299 cells (**a**, **c**, **d**) are normalized to the levels of apoptosis in mock-transfected cells (0%).

Mdm2, indicating that the structure of *p53* mRNA is essential for binding to Mdm2 (Fig. 2e). Consistent with this, we found that the L22L mutation, which does not change the predicted secondary structure of the MBD-ES (Supplementary Information, Fig. S1a; ref. 16), only affected Mdm2 binding when introduced into *p53* mRNA and not into the MBD-ES oligonucleotide (compare Fig. 2e with Supplementary Information, Fig. S4c). Furthermore, the phenotype of $p53^{L22L}$ mRNA was reversed after introduction of a second silent mutation in an adjacent RNA structure (Supplementary Information, Fig. S4d). These results, together with the finding that Mdm2 interacts with small non-specific RNA oligonucleotides, suggest that a single silent mutation can affect the tertiary structure of the *p53* mRNA and, in this way, the interaction with an oligonucleotide binding pocket in Mdm2.

The observation that the non-RNA binding Mdm2 mutant G446S is less effective in inducing *p53* translation (Fig. 2f) indicates that the direct Mdm2–*p53* mRNA interaction controls the rate of p53 synthesis. This is supported by the finding that $p53^{STriM}$ RNA prevented Mdm2 from promoting translation of wild-type *p53* mRNA (Fig. 2f), presumably by competing with it for binding to Mdm2 (Fig. 2a). Furthermore, in the presence of *p53* mRNA, wild-type Mdm2 was found in the polysomal fractions in larger amounts than $Mdm2^{G446S}$ (Fig. 2g), suggesting that wild-type Mdm2, but not the non-RNA binding Mdm2, is associated with translating mRNA.

As deletion of the N terminus of Mdm2 seems to strengthen the interaction with *p53* mRNA, we next tested whether the interaction between the Mdm2 and p53 proteins interferes with Mdm2 binding to *p53* mRNA, or whether *p53* mRNA affects the Mdm2–p53 protein–protein interaction. However, increasing the amounts of p53 protein expressed in H1299 cells did not seem to prevent the interaction between Mdm2 and *p53* mRNA (Fig. 3a), and increasing the amounts of $p53^{STriM}$ mRNA augmented Mdm2 and p53 levels without affecting the Mdm2–p53 protein interaction (Fig. 3b). Hence, these data do not support the idea that *p53* mRNA competes with p53 protein for binding to Mdm2 but instead suggest that Mdm2 may bind the p53 protein and mRNA simultaneously through its N- and C-terminal domains, respectively.

The observed increase in Mdm2 levels caused by $p53^{STriM}$ mRNA (Fig. 3b) does not require the p53 protein, whereas the increase in p53 levels is Mdm2-dependent (Fig. 3c). The effect on wild-type Mdm2 expression levels did not occur with the E3 ligase mutant $Mdm2^{C464A}$ or with the non-RNA-binding Mdm^{2G446S} (Fig. 3c). The effect of non-coding $p53^{S}$ mRNAs on p53 levels correlates with the binding affinity of the respective RNA to Mdm2 (Fig. 3c). The data shown in Fig. 3b and c suggest that binding of *p53* mRNA to the RING domain of Mdm2 inhibits its auto-[17] and hetero-ubiquitination capacity, and the subsequent degradation of p53 and Mdm2. In support of this, we found that $p53^{STriM}$ mRNA suppressed Mdm2-dependent ubiquitination of p53 more efficiently than $p53^{SL22L}$ mRNA (Fig. 3d; Supplementary Information, Fig. S2), and that Mdm2 levels were higher when p53 was expressed from the *TriM* mRNA and lower in the presence of *L22L* (Fig. 3e; Supplementary Information, Fig. S3b). p53 is known to induce *Mdm2* gene transcription[18] and these results show that *p53* mRNA can also increase Mdm2 levels, probably by controlling its E3 ligase activity. Hence, just as Mdm2 has a dual effect on p53 expression, both the p53 protein and the p53 mRNA can regulate Mdm2 levels.

As Mdm2 controls p53 activity, we next set out to test whether *p53* mRNA also affects Mdm2-dependent control of p53-induced apoptosis. As expected, we found that expression of Mdm2 reduced the pro-apoptotic activity of p53 in H1299 cells. Co-expression of $p53^{STriM}$ mRNA overcame this inhibition (Fig. 4a) but this did not occur in cells expressing the non-RNA binding Mdm2 ($Mdm2^{G446S}$). This indicates that the pro-apoptotic activity of $p53^{STriM}$ mRNA is dependent on its capacity to interact with Mdm2. Similarly, expression of $p53^{STriM}$ mRNA, but not a non-coding $p53^{S}$ mRNA, in which the first 120 coding nucleotides have been deleted (SΔ120), prevented Mdm2 from suppressing apoptosis in the human sarcoma-derived MLS-1765 cell line[6], which expresses endogenous p53 (Fig. 4b). As with H1299 cells expressing exogenous p53, $p53^{STriM}$ mRNA caused an increase in the endogenous levels of p53 in an Mdm2-dependent manner in MLS-1765 and human breast adenocarcinoma MCF-7 cells (Supplementary Information, Fig. S5a).

Hence, $p53^{S}$ mRNAs affect Mdm2-dependent control of p53 activity and we next tested whether this is also the case for p53-encoding mRNAs. We investigated the effects of mutations in Ser 15 and Ser 20 of p53 as these are located in the MBD-ES region and there is divided opinion on the importance of these phosphorylation sites in controlling p53 activity[19–21]. When we introduced silent mutations (Ser 15 Ser and Ser 20 Ser) that mimic the predicted changes in the MBD-ES structure caused by the alanine substitutions commonly used to study the importance of these residues (Supplementary Information, Fig. S1a), we found that the silent mutations and alanine substitutions had the same effect on p53 function (Fig. 4c). This suggests that the nucleotide substitutions, and not the changes in amino acids, are responsible for the effect on p53 activity previously attributed to amino acids 15 and 20. Similarly, the pro-apoptotic activity of wild-type p53 protein expressed from *L22L*, or from two other single silent cancer-derived p53 mutations (V10V[22] and P36P[23]; GTC>GTT and CCG>CCT, respectively) was reduced (Fig. 4c). These mRNAs have reduced affinity for Mdm2 and, consequently, express lower levels of p53 protein (Supplementary Information, Fig. S5b, c).

Our results indicate that the effect of *p53* mRNA on p53 activity is mediated by Mdm2 and to confirm this we compared the pro-apoptotic effect of $p53^{TriM}$, wild-type and $p53^{L22L}$ mRNAs at different levels of Mdm2 expression. Expression of p53 protein from each of these mRNAs resulted in similarly high levels of apoptosis when endogenous *Mdm2* was knocked down using siRNA (Fig. 4d; Supplementary Information, Fig. S3b). Under conditions of endogenous Mdm2 expression, the level of apoptosis was significantly reduced when p53 was expressed from the *L22L* message. When levels of Mdm2 increased after overexpression, *L22L*-derived p53 did not induce apoptosis above background, whereas the activity of $p53^{TriM}$ remained high. Importantly, in the presence of the non-RNA binding $Mdm2^{G446S}$, $p53^{TriM}$ mRNA lost its capacity to prevent Mdm2-mediated inhibition of apoptosis. Thus, the affinity of *p53* mRNA for Mdm2 determines the levels of Mdm2-dependent suppression of p53-induced apoptosis.

Taken together, our results show that Mdm2 binding to *p53* mRNA causes accumulation of Mdm2 at the polysome, stimulation of p53 synthesis and inhibition of the E3 ligase activity of Mdm2. We propose that release of the p53–Mdm2 protein complex from the polysome activates the E3 ligase activity of Mdm2. This would explain why the increase in the affinity of *p53* mRNA to Mdm2 augments the rate of p53 synthesis and degradation (Fig. 1a; Supplementary Information, Fig. S2a). This also explains how a weakening in the Mdm2–*p53* mRNA interaction results in an increase in Mdm2-dependent suppression of p53 pro-apoptotic activity. In this model, *p53* mRNA acts as a switch controlling the function of Mdm2 towards p53 (Fig. 4e)[4,24].

The finding that the capacity of Mdm2 to control p53 synthesis and degradation emerge from the same genomic sequences in both *mdm2* and *p53* indicates that these functions have evolved together and it is plausible that the interaction between *p53* mRNA and Mdm2 forms the basis for the development of an intricate p53–Mdm2 feedback system[25]. These results are consistent with a mechanism by which single silent nucleotide changes within the coding region of an mRNA can affect the activity of the encoded protein by controlling the function of its regulator. □

METHODS

Protein labelling and expression. All cell-based assays were carried out in *p53*-null H1299 cells, except for experiments in Fig. 4b, in which the MLS-1765 cells expressing endogenous wild-type p53 were used. For all experiments, transfection efficiency and mRNA levels were verified using real-time quantitative reverse transcription PCR (qRT–PCR). ^{35}S-methionine labelling was carried out by culturing the cells in methionine-free medium containing 2% dialysed fetal calf serum (FCS) for 1 h and proteasome inhibitor MG132 (22 μM, Merck Biosciences). Easytag Express Protein Labeling Mix (^{35}S, 90 μCi; PerkinElmer) was added for 20 min, and p53 proteins were immunoprecipitated using CM-1 antibody (a gift from B. Vojtesek, Masaryk Memorial Cancer Institute, Brno, Czech Republic) and separated by SDS–PAGE. *In vitro* translation was performed for one of the *in vitro* ubiquitination assays using the rabbit reticulocyte lysate system (Promega) and *in vitro* transcribed capped mRNA (Ambion) according to the manufacturer's protocols. Quantification of radioactively labelled products was determined using phosphoimager (Amersham) and Storm hardware together with Bio-1D software (Vilber-Lourmat). Cells were treated with cycloheximide

(CHX, 10 μg ml^{-1}) for 1 h. Treatment with doxorubicin (0.1 μM) and tunicamycin (1.2 μM), or an equal volume of dimethylsuphoxide (DMSO) was for 16 h.

Quantitative RNA co-immunoprecipitation (qRNAco-IP). qRNAco-IP assays were based on a previous protocol[26]. Briefly, transfected H1299 cells were lysed with buffer containing RNase OUT (100 U ml^{-1}, Invitrogen), centrifuged, and supernatants were pre-cleared with mouse IgG followed by incubation with the monoclonal anti-Mdm2 antibody SMP14 (a gift from B. Vojtesek) directed against amino acids 154–167 of Mdm2 present in all deletion mutants tested (the monoclonal anti-Mdm2 antibody 4B2 was also used in experiments where wild-type Mdm2 alone was immunoprecipitated). The complexes were pulled down using protein G beads (Amersham), treated with proteinase K (Sigma) and RNA was extracted and purified using TRIzol protocol (Invitrogen). qRT–PCR was performed using primers against *p53* and control genes TATA Box-binding protein and β-actin. To ensure valid quantification of RNA binding to Mdm2, standard curves were used to test for efficiency of transfection, RT–PCR and qPCR protocols. qRT–PCRs on total RNA were performed and qRNAco-IP values calculated according to the formula: (qPCR value *p53* mRNA IP/qPCR value *p53* mRNA total)/(qPCRvalue control mRNA IP/qPCR value control mRNA total). A western blot using anti-Mdm2 antibody was performed in parallel and co-immunoprecipitation data were normalized to total Mdm2 protein when needed.

***In vitro* quantitative RNA co-immunoprecipitation (*in vitro* qRNAco-IP).** All binding reactions were carried out for 10 min at 37 °C in binding buffer containing 50 mM Tris pH 7.5, 150 mM NaCl, 0.02 mg ml^{-1} yeast tRNA, 0.2 mg ml^{-1} BSA. hMdm2 protein (120 ng) purified from insect cells, and wild-type or mutated *p53* mRNA (8.10^{-3} pmol) were used. As a control, wild-type *p53* mRNA was heated for 4 min at 98 °C, before the binding reaction. Various amounts (ranging from 0 to 40 fmol) of competitor RNA corresponding to the Mdm2 binding site of *p53* (5′-gtcaggaaacattttcagacctatggaaactacttcctgaaa-3′) were also added to the binding reaction.

The RNA–protein complexes were pulled down using a monoclonal anti-Mdm2 antibody 4B2 (a gift from B. Vojtesek) and protein G beads (Amersham). The unbound fraction was recovered for later analysis and the bound RNA was treated with proteinase K (Sigma). The bound and free RNA fractions were then extracted and purified using TRIzol protocol (Invitrogen). qRT–PCR was performed on these fractions using primers against *p53* that recognize *p53* mRNA only and not the competitor oligonucleotide. The binding results were expressed as a ratio between the bound and the total (bound + free) RNA.

Trimolecular fluorescence complementation (TriFC). In this system, a portion of the Venus fluorescent protein[15] is tethered to *p53* mRNA by the bacteriophage MS2 coat protein–RNA operator interaction[27]. The complementary portion of Venus is fused to different Mdm2 mutants as indicated. If Mdm2 is able to associate with *p53* mRNA, it will bring the two portions of Venus in close proximity to form a fluorescent complex, while simultaneously identifying their site of interaction within the cell. H1299 cells were transfected with the three constructs and observed after 48 h using a reversed confocal microscope according to standard methods. Red fluorescent protein was used as a transfection control and the cell nucleus were stained with DAPI.

Electrophoretic mobility shift assay (EMSA). EMSA was performed essentially as previously described[28]. Both bacterially and insect-expressed and purified hMdm2 were used in an RNA-binding reaction with a biotin-labelled RNA sequence containing the Mdm2 binding domain-encoding sequence (MBD-ES, nucleotides 45–78). Reaction mixtures (20 μl) contained 50 mM Tris–HCl pH 7.0, 150 mM NaCl, 0.25 mg ml^{-1} tRNA (Ambion), 0.25 ml^{-1} bovine serum albumin (Sigma), 1 pmol biotin-labelled RNA (Eurogentec) and 150 ng hMdm2 and 2 pmol *in vitro*-transcribed *p53* mRNA (Ambion, MessageMachine) when indicated. Mixtures were incubated at 37 °C for 10 min. After incubation, dye mixture (4 μl, Gel Loading buf II, Ambion) was added and the samples were immediately loaded on a 6% DNA retardation gel (Invitrogen) in 0.5 × TBE. Electrophoresis was carried out at 70 V at room temperature for 45 min and RNA complexes were transferred (northern blotting) to N$^+$ Hybond filter (Amersham), fixed, blocked and washed before being visualized using HRP-conjugated streptavidin. The bands were quantified using ECL, CCD camera and Bio-1D software (Vilber-Lourmat).

Ubiquitination assays. For *in vivo* ubiquitination assays, H1299 cells were treated with the proteasome inhibitor MG-132 36 h after transfection and lysed. Cell lysates were used for direct western blot analysis using CM-1 antibody.

In vitro ubiquitination assays were performed according to two different protocols. The fist was a modification of a protocol used previously[29]. Rabbit reticulocyte lysate (2 μl, Promega)-translated ^{35}S-labelled p53 was incubated in the presence of E1 (50 ng, Calbiochem), UbcH5 (50 ng, Calbiochem) and yeast tRNA (10 μg, Ambion) in 50 μl volumes of reaction buffer containing 25 mM Tris-HCl (pH 7.5), 100 mM NaCl, 1 mM dithiothreitol, 2 mM ATP and 4 mM MgCl2. His-ubiquitin (10 μg, Calbiochem), bacterially expressed hMdm2 (400 ng) and *in vitro*-transcribed *p53* mRNA (3 μg, Ambion, MessageMachine) was added as indicated. After incubation at 30 °C for 2 h, reactions were stopped and separated over a 4–12% Bis-Tris NuPage gel (Invitrogen). ^{35}S-labelled substrates were detected and quantified using phosphoimager (Supplementary Information, Fig. S5). For the second protocol[30], immunoprecipitated p53 expressed in H1299 cells was used instead of *in vitro* translated p53, and hMdm2 expressed by insect cells instead of bacterially expressed hMdm2. The data were analysed by western blotting using antibodies against p53 (CM-1, 1:7000) and His-ubiquitin (anti-His-HRP, 1:10,000; Clontech) (Fig. 3d).

Flow cytometry. The percentage of apoptotic cells in a population was measured as described previously[31]. Briefly, transfected cells were stained with annexin V-FITC and propidium iodide (PI) (annexin V-FITC apoptosis detection kit; Sigma) and analysed by flow cytometry with an LSR flow cytometer and CellQuest software (Becton-Dickinson). The test discriminates between intact cells (FITC–/PI–), apoptotic cells (FITC+/PI–) and necrotic cells (FITC+/PI+).

Note: Supplementary Information is available on the Nature Cell Biology website.

ACKNOWLEDGEMENTS

This work was supported by AICR, AVENIR/INSERM and La Ligue Contre le Cancer. M.M.C. was supported by grant SFRH/BD/16697/2004 from the Fundação para a Ciência e a Tecnologia of Portugal. Bacterial purified hMdm2 was a gift from D. Xirodimas and we are thankful to Chris M. Brown and Nattanan Panjaworayan, Dunedin, New Zealand for providing the TriFC constructs. Anti-p53 and anti-Mdm2 antibodies were a gift from B. Vojtesek. Flow cytometry and immunofluorescence microscopy experiments were performed at the Imagery Department of the Institut Universitaire d'Hematologie-IFR105.

AUTHOR CONTRIBUTIONS

R.F. and M.M.C. designed the project; M.M.C., L.M.-C. and M.M.M. performed the experiments; all authors contributed to data analysis; R.F., M.M.C. and C.D. wrote the manuscript.

COMPETING FINANCIAL INTERESTS

The authors declare no competing financial interests.

Published online at http://www.nature.com/naturecellbiology/
Reprints and permissions information is available online at http://npg.nature.com/reprintsandpermissions/

1. Zhu, J., Zhou, W., Jiang, J. & Chen, X. Identification of a novel p53functional domain that is necessary for mediating apoptosis. *J. Biol. Chem.* **273,** 13030–13036 (1998).
2. Kubbutat, M. H., Jones, S. N. & Vousden, K. H. Regulation of p53 stability by Mdm2. *Nature* **387,** 299–303 (1997).
3. Haupt, Y., Maya, R., Kazaz, A. & Oren, M. Mdm2 promotes the rapid degradation of p53. *Nature* **387,** 296–299 (1997).
4. Yin, Y., Stephen, C. W., Luciani, M. G. & Fahraeus, R. p53 Stability and activity is regulated by Mdm2-mediated induction of alternative p53 translation products. *Nature Cell Biol.* **4,** 462–467 (2002).
5. Kussie, P. H. *et al.* Structure of the MDM2 oncoprotein bound to the p53 tumor suppressor transactivation domain. *Science* **274,** 948–953 (1996).
6. Candeias, M. M. *et al.* Expression of p53 and p53/47 are controlled by alternative mechanisms of messenger RNA translation initiation. *Oncogene* **25,** 6936–6947 (2006).
7. Ray, P. S., Grover, R. & Das, S. Two internal ribosome entry sites mediate the translation of p53 isoforms. *EMBO Rep.* **7,** 404–410 (2006).
8. Honda, R., Tanaka, H. & Yasuda, H. Oncoprotein MDM2 is a ubiquitin ligase E3 for tumor suppressor p53. *FEBS Lett.* **420,** 25–27 (1997).
9. Oscier, D. G. *et al.* Multivariate analysis of prognostic factors in CLL: clinical stage, IGVH gene mutational status, and loss or mutation of the p53 gene are independent prognostic factors. *Blood* **100,** 1177–1184 (2002).
10. Perry, M. E. Mdm2 in the response to radiation. *Mol. Cancer Res.* **2,** 9–19 (2004).
11. Cheng, T. H. & Cohen, S. N. Human MDM2 isoforms translated differentially on constitutive versus p53-regulated transcripts have distinct functions in the p53/MDM2 and TSG101/MDM2 feedback control loops. *Mol. Cell Biol.* **27,** 111–119 (2007).

12. Marechal, V., Elenbaas, B., Piette, J., Nicolas, J. C. & Levine, A. J. The ribosomal L5 protein is associated with mdm-2 and mdm-2-p53 complexes. *Mol. Cell Biol.* **14,** 7414–7420 (1994).
13. Elenbaas, B., Dobbelstein, M., Roth, J., Shenk, T. & Levine, A. J. The MDM2 oncoprotein binds specifically to RNA through its RING finger domain. *Mol. Med.* **2,** 439–451 (1996).
14. Rackham, O. & Brown, C. M. Visualization of RNA-protein interactions in living cells: FMRP and IMP1 interact on mRNAs. *EMBO J.* **23,** 3346–3355 (2004).
15. Nagai, T. *et al.* A variant of yellow fluorescent protein with fast and efficient maturation for cell-biological applications. *Nature Biotechnol.* **20,** 87–90 (2002).
16. Mathews, D. H., Sabina, J., Zuker, M. & Turner, D. H. Expanded sequence dependence of thermodynamic parameters improves prediction of RNA secondary structure. *J. Mol. Biol.* **288,** 911–940 (1999).
17. Fang, S., Jensen, J. P., Ludwig, R. L., Vousden, K. H. & Weissman, A. M. Mdm2 is a RING finger-dependent ubiquitin protein ligase for itself and p53. *J. Biol. Chem.* **275,** 8945–8951 (2000).
18. Juven, T., Barak, Y., Zauberman, A., George, D. L. & Oren, M. Wild type p53 can mediate sequence-specific transactivation of an internal promoter within the *mdm2* gene. *Oncogene* **8,** 3411–3416 (1993).
19. Unger, T. *et al.* Mutations in serines 15 and 20 of human p53 impair its apoptotic activity. *Oncogene* **18,** 3205–3212 (1999).
20. Dumaz, N. & Meek, D. W. Serine 15 phosphorylation stimulates p53 transactivation but does not directly influence interaction with HDM2. *EMBO J.* **18,** 7002–7010 (1999).
21. Thompson, T. *et al.* Phosphorylation of p53 on key serines is dispensable for transcriptional activation and apoptosis. *J. Biol. Chem.* **279,** 53015–53022 (2004).
22. Hayes, V. M. *et al.* Comprehensive TP53-denaturing gradient gel electrophoresis mutation detection assay also applicable to archival paraffin-embedded tissue. *Diagn. Mol. Pathol.* **8,** 2–10 (1999).
23. Kanjilal, S. *et al.* p53 mutations in nonmelanoma skin cancer of the head and neck: molecular evidence for field cancerization. *Cancer Res.* **55,** 3604–3609 (1995).
24. Fahraeus, R. Do peptides control their own birth and death? *Nature Rev. Mol. Cell Biol.* **6,** 263–267 (2005).
25. Jin, S. & Levine, A. J. The p53 functional circuit. *J. Cell Sci.* **114,** 4139–4140 (2001).
26. Tenenbaum, S. A., Lager, P. J., Carson, C. C. & Keene, J. D. Ribonomics: identifying mRNA subsets in mRNP complexes using antibodies to RNA-binding proteins and genomic arrays. *Methods* **26,** 191–198 (2002).
27. Lima, S. M., Peabody, D. S., Silva, J. L. & de Oliveira, A. C. Mutations in the hydrophobic core and in the protein-RNA interface affect the packing and stability of icosahedral viruses. *Eur. J. Biochem.* **271,** 135–145 (2004).
28. Li, Y., Jiang, Z., Chen, H. & Ma, W. J. A modified quantitative EMSA and its application in the study of RNA--protein interactions. *J. Biochem. Biophys. Methods* **60,** 85–96 (2004).
29. Jaffray, E. G. & Hay, R. T. Detection of modification by ubiquitin-like proteins. *Methods* **38,** 35–38 (2006).
30. Rodriguez, M. S. *et al.* SUMO-1 modification activates the transcriptional response of p53. *EMBO J.* **18,** 6455–6461 (1999).
31. Vermes, I., Haanen, C., Steffens-Nakken, H. & Reutelingsperger, C. A novel assay for apoptosis. Flow cytometric detection of phosphatidylserine expression on early apoptotic cells using fluorescein labelled annexin V. *J. Immunol. Methods* **184,** 39–51 (1995).